Efficacité de la représentation temps-fréquence pour expliquer l'effet de la symétrie dans la propagation des vibrations élastiques autour d'un tube

S Agounad, E H Aassif, Y Khandouch, G. Maze

CFA/VISHNO 2016

Efficacité de la représentation temps-fréquence pour expliquer l'effet de la symétrie dans la propagation des vibrations élastiques autour d'un tube

S. Agounad[a], E.H. Aassif[a], Y. Khandouch[a] et G. Maze[b]
[a]Département de physique, Université Ibn Zohr, Agadir, 80060 Agadir, Maroc
[b]LOMC UMR CNRS 6294, Université du Havre, 75 rue Bellot, 76600 Le Havre, France
said.agounad@edu.uiz.ac.ma

The excitation of onelayer elastic tube, submerged in water and air-filled cavity, perpendicularly to its revolution axis, gives rise to the propagation of several wave types. This phenomena calls scattering acoustic. Generally, the generated waves are divided into two categories, specular echo and elastic waves. Basing on the study of the elastic waves, allows us on one hand to study the scattering acoustic and on the other hand to extract the relevant features required to characterize the target. The analysing of the time and frequency representations of the backscattering acoustic pressure by the tube, under normal incidence, for different values of the azimuthal angle between 0° and 180°, shows that this pressure is varied as function of this angle. These representations reveal the variation of the elastic waves constituting the backscattering pressure but are not adequate to give the convincing explanation of this variation. In order to explain this variation we appealed the time-frequency representation. Among time-frequency representations the spectrogram (SP), the smoothing pseudo Wigner-Ville (SPWV) and the reassigned SPWV (RSPWV) are used in this work. The application of these representations on the backscattering acoustic pressure for different azimuthal angle values, we lead to find the explication of the variation of this pressure as a function of the azimuthal angle.

1 Introduction

The application of the ultrasonic technique in different fields such as acoustic characterization, nondestructive testing (NDT) and identification, has received a lot of interest [1–3]. The characterization and the identification of an elastic tube using this technique have seen numerous theoretical and experimental searches [4–8]. The principle of the ultrasonic technique consist to excite the elastic tube normally or obliquely by an incident plane wave, the scattering acoustic phenomena is observed and then the backscattering waves are detected. The theoretical model is developed to study and understand the acoustic scattering [6,9]. This model is based on the resolution of the wave propagation equation and boundary conditions of the stress and displacement tensor [6]. The resonant scattering theory (RST) [4, 9] has used to observe and explain the resonances. On the other hand many experimental methods have been proposed to verify the theoretical results such as the method of identification and isolation of resonances (MIIR) [6, 8]. The method MIIR consists on one hand to isolate the resonances using the resonance spectrum (monstatic method), and on the other hand is aimed to identify the vibration modes n of the resonances of the circumferential waves (bistatic method).

The studying of the time and frequency representations of the scattering acoustic by the elastic monolayer tube immersed in water demonstrates the existence of two wave types, the specular echo which is characterized by large amplitude and short duration, and the elastic waves with short amplitude and large duration. The elastic waves are divided into symmetric (S_i, $i = 0, 1...$) and antisymmetric (A, A_i) circumferential waves [10–12]. The propagation of the elastic waves around the peripheral of the tube creates the standing waves. The resonances as a consequence of these waves. The resonance spectrum is used to observe and analyse of the resonances which are noted by (n,l) with n is the vibration mode and l is the type of wave.

The time-frequency representation has suggested to overcome the drawbacks of the time and frequency analysis. This technique allows jointly the analysis in time and frequency, moreover the time-frequency methods present very important properties such as the time group delay and the instantaneous frequency which are used to compute the group and phase velocities of circumferential waves.

Numerous time-frequency techniques have been developed [14–16]. The spectrogram (SP), Wigner-Ville distribution (WVD) and its variant smoothed pseudo Wigner-Ville (SPWV) are the most interesting time-frequency methods. To ameliorate the time-frequency representation, the reassignment techniques have been proposed [18, 19]. The reassigned smoothed pseudo Wigner-Ville (RSPWV) method is used in this work to study the scattering acoustic phenomena. In acoustic the time-frequency representation has already used to study the backscattering acoustic pressure by an elastic tube, under normal incidence and for an azimuthal angle equal 180° (reception angle) [2]. In this work we proposed to use the time-frequency method to analyze the scattering acoustic as a function of different values of azimuthal angle (θ). By reason of the symmetry the study of the scattering acoustic for θ varied from 0° to 360° can be assimilated to the study for θ varied from 0° to 180°.

The remainder of the paper is structured as follows. The principle of the acoustic scattering by an elastic tube and its analyse in time and frequency domain are depicted in section 2. The section 3 depicts the comparison of some time-frequency methods. In the section 4 we reveal the time-frequency content for different values of reception angle. Finally, section 5 outlines conclusions.

2 Scattering acoustic by an elastic tube

2.1 Form function

To characterize and identify an elastic tube using the ultrasonic technique, the tube of radii ratio b/a (b and a is the inner and outer radius), immersed in water (or in another fluid) where the acoustic wave is propagated with the velocity c_1 and air-filled cavity. The piezoelectric transducer emitters an incident wave of wave vector k_1, exciting the tube perpendicularly to its axis. The acoustic scattering phenomena of this wave is observed. The receptor transducer placed in point $M(\rho, \theta)$ records the backscattering acoustic waves figure 1.

The study of the backscattering acoustic pressure in normal incidence by the tube shows that the following waves are generated: the specular echo, the interface wave (wave A) and the surface waves (Rayleigh l=1, whispering gallery l>1,...) [9, 11, 12]. Basing on the boundary conditions at the interfaces ($\rho = a$, $\rho = b$) of the tube and resolution of wave propagation equation [9], The radiating pressure in normal incident can be expressed using the form function in far field f_∞ [6, 9], this function is as a function of reduced frequency

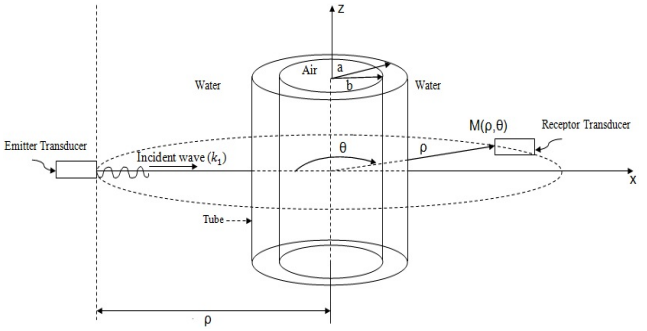

Figure 1: Scattering acoustic by an elastic tube. Incidence wave arrived with $\gamma = 0$; The point M of pressure field resulting is marked by cylindrical coordinate system (ρ, θ).

x_1 ($x_1 = k_1 a$) and azimuthal angle θ:

$$f_\infty(x_1, \theta) = \frac{2}{\sqrt{\pi x_1}} \left| \sum_{n=0}^{\infty} \epsilon_n \frac{D_n^{[1]}(a,b)}{D_n(a,b)} cos(n\theta) \right| \qquad (1)$$

where ϵ_n is the Neumann coefficient, D_n and $D_n^{[1]}$ are two determinants calculated from the continuity conditions.

The figure 2 represents the form function in far field of the Aluminum tube (b/a=0.95, $c_L = 6380m/s$, $c_T = 3600m/s$ and $\rho_2 = 2790kg/m^3$) immersed in water ($c_1 = 1470$, $\rho_1 = 1000kg/m^3$) and the air-filled cavity ($c_3 = 334m/s$, $\rho_3 = 1.29kg/m^3$).

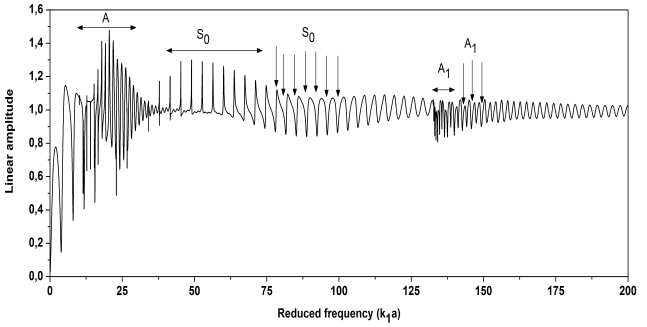

Figure 2: The Form function for the submerged Aluminum tube (b/a=0.95) and air-filled cavity, $\gamma = 0$.

2.2 Impulse response

The form function is as a function of reduced frequency x_1, to obtain an evolution chronological of acoustic scattering the Inverse Fourier Transform is applied on the form function as follows:

$$p_{scat}(t) = \frac{1}{2\pi} \int_{-\infty}^{+\infty} f(x_1) f_\infty(x_1, \theta) e^{(jx_1 t)} dx_1 \qquad (2)$$

where $f(x_1)$ is the bandpass of the transducer, generally is approximated by hamming function.

The temporal signal for the immersed Aluminum tube (b/a=0.95) in water and air-filled cavity is illustrated on the figure 3.a. On this figure two intervals are observed, first characterises by the large amplitude (specular echo) and the second characterizes by the short amplitude (elastic waves). The last interval appears the succession of the associated wavepackets to the elastic waves which are at the beginning, more or less easier to identify but in the last moment, these wavepackets are finished by overlapping, and consequently their identification is becoming trickier.

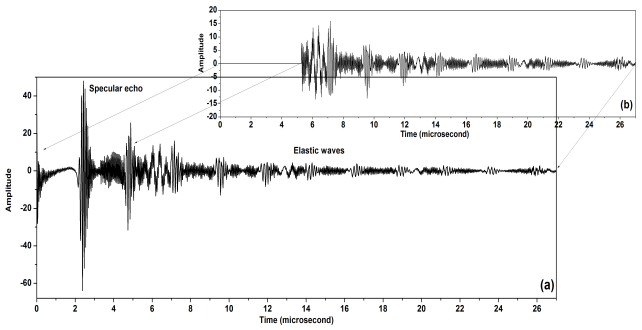

Figure 3: (a) Impulse response for the Aluminum tube (b/a=0.95). (b) Impulse response without specular echo.

2.3 Resonance spectrum and modal isolation plan

The analysing of the backscattering acoustic pressure in frequency domain is based on the studying of the resonances of the elastic waves. The resonance spectrum is obtained from the impulse response. Suppressing the non resonant part of the impulse response fig.3.a, then the application of the Fourier Transform on the new signal fig.3.b allows to obtained the resonance spectrum. The figure 4 shows this spectrum of the submerged aluminum tube (b/a=0.95).

The used range of reduced frequency is $0 < x_1 < 200$. In this range, the resonance frequencies of wave A are observed for $x_1 < 30$, the resonances of wave S_0 are appeared for $30 < x_1 < 94$ and those of A_1 are observed for $130 < x_1 < 140$.

The peaks observed on the resonance spectrum fig.4 are linked to the resonance frequencies of vibration modes n of elastic waves. The vibration mode n for each resonance is the number of wavelengths of a circumferential wave around the circumference of the tube. The resonance spectrum has already calculated is the outcome of the summation of the vibration modes n for each frequency, during the calculation of the form function. Then an other representation can be used to analyze the resonances is to represent the mode n as a function of reduced frequency x_1. This representation is called modal isolation plan. The figure 4.b depicts the modal isolation plan associated to the resonance spectrum for the Aluminum tube (b/a=0.95). This figure shows that the waves

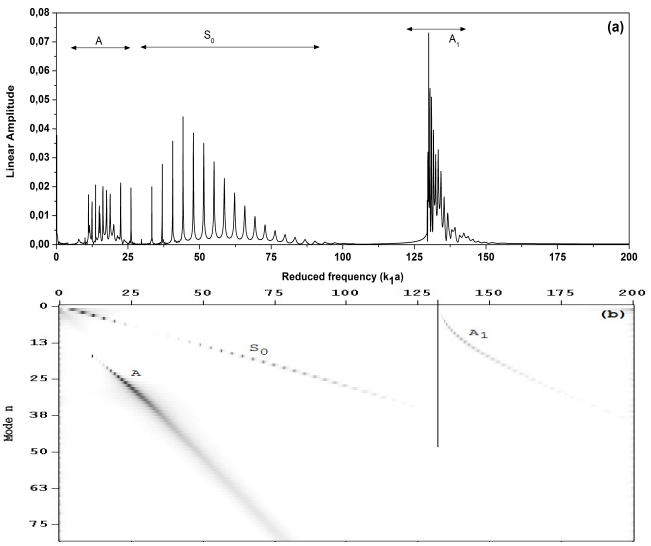

Figure 4: (a) Resonance spectrum, (b) Modal isolation plan, for the submerged Aluminum tube (b/a=0.95), $\gamma = 0$

A and S_0 haven't the reduced cutoff frequency, while that of the A_1 wave is indicated by the vertical asymptotic of the trajectory of this wave fig.4.b.

3 Time-frequency representation

So far, we have studied the scattering acoustic using the time and frequency analysis, to overcome the limitations of these types of analysis and for further analysis we use the time-frequency technique. This technique allows the deepen analysis jointly in time and frequency [14–16].

3.1 Spectrogram distribution

The short time Fourier Transform (STFT) has suggested to surmount the limitations of Fourier Transform [14, 16]. The STFT of a signal $x(t)$ is expressed by:

$$STFT_x^h(t,\nu) = \int_{-\infty}^{+\infty} x(\tau)h^*(\tau - t)e^{(-2\pi j\nu\tau)}d\tau \qquad (3)$$

The spectrogram (SP) is defined as the energy density, for the signal $x(t)$, is calculated as the square modulus of its STFT [14, 16]:

$$SP_x(t,\nu) = \left|STFT_x^h(t,\nu)\right|^2 \qquad (4)$$

3.2 Smoothed Pseudo Wigner-Ville (SPWV)

The SPWV is the variant of the Wigner-Ville distribution. The SPWV has been proposed to reduce the interference terms appeared between the own components of the analysing signal in time-frequency plane of Wigner-Ville distribution. This method is written as follows:

$$SPWV_{x_a}^{g,h}(t,\nu) = \int_{-\infty}^{+\infty} h(\tau)\int_{-\infty}^{+\infty} g(\mu)x_a(t-\mu+\tau/2) \times x_a^*(t-\mu-\tau/2)e^{(-2\pi j\nu\tau)}dtd\mu \qquad (5)$$

where the signal x_a is the analytic signal of the analysing signal. The windows g and h are two real windows.

3.3 Reassignment SPWV (RSPWV) distribution

The reassignment technique has been developed to ameliorate the readability of the time-frequency representation. For it, some authors [18, 19] suggested to assign each value to the centre of gravity of the cell's energy, whose coordinates ($\hat{t}$,$\hat{\omega}$) are computed by the following expressions:

$$\hat{t}_{xa}(t,\omega) = t - \frac{SPWV_{x_a}^{\tau g,h}(t,\omega)}{SPWV_{x_a}^{g,h}(t,\omega)} \qquad (6)$$

$$\hat{\omega}_{xa}(t,\omega) = \omega + j\frac{SPWV_{x_a}^{g,Dh}(t,\omega)}{SPWV_{x_a}^{g,h}(t,\omega)} \qquad (7)$$

where the windows τh and Dh are two smoothing windows obtained from the window $h(t)$.

$$RSPWV_{x_a}(t',\omega') = \int\int SPWV_{x_a}^{g,h}(t,\omega)\delta(t' - \hat{t}(t,\omega)) \times \delta(\omega' - \hat{\omega}(t,\omega))\frac{dtd\omega}{2\pi} \qquad (8)$$

3.4 Application and comparison of SP, SPWV and RSPWV on acoustic scattering

This section is dedicated to apply and compare the time-frequency representations those we have already presented. The figure 5 shows the spectrogram time-frequency representation for the aluminum tube (b/a=0.95) obtained from the temporal signal without specular echo fig.2.b. The SPWV and RSPWV time-frequency images are represented respectively on the figures 6.a and 6.b.

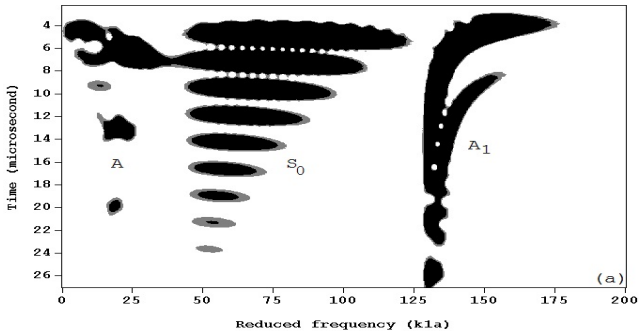

Figure 5: SP image of the Alumminum tube (b/a=0.95), $\theta = 180°$

The analysing of different time-frequency representations on reduced frequency range $0.1 < k_1a < 200$, shows that the time signal for the aluminum tube is the result of the contribution of three circumferential waves A, S_0 and A_1. We observe that these waves are less or more localized in time-frequency plane. The evolution of the wave A is observed in the range of reduced frequencies lower than 33, the wave S_0 is appeared for the reduced frequencies varied between 40 and 120 and the wave A_1 is beginning to exist for the reduced frequencies higher than 130.

The fig. 5 shows, on one hand that the spectrogram provides the time-frequency image without the interference terms but on the other hand is suffered from the broadening spectrum problem. On the SPWV time-frequency image we observe the better localization than the spectrogram but is presented some interference terms which sometime may be influenced the readability of image. The fig. 6.b shows that the RSPWV offers less interference terms and more concentration of the wave trajectories than SPWV and SP.

4 Evolution of the backscattering acoustic pressure as a function of angle θ

In this section we are going to present the time-frequency analysis for the backscattering acoustic pressure as a function of azimuthal angle θ. According to the symmetry reasons [6, 9], in this work the time-frequency analysis is applied for the calculated backscattering pressure between $\theta = 0°$ and $\theta = 180°$ in $10°$ steps. This analysis reveals that the evolution of the time-frequency plane of the backscattering pressure from $\theta = 180°$ to $\theta = 90°$ is as the same as this plane for $\theta = 0°$ to $\theta = 90°$. The figures 6 to 15 show the SPWV and RSPWV images of the backscattering acoustic pressure for the Aluminum tube (b/a=0.95) and for the azimuthal angle varied between $\theta = 180°$ and $\theta = 0°$ in $\theta = 10°$ steps.

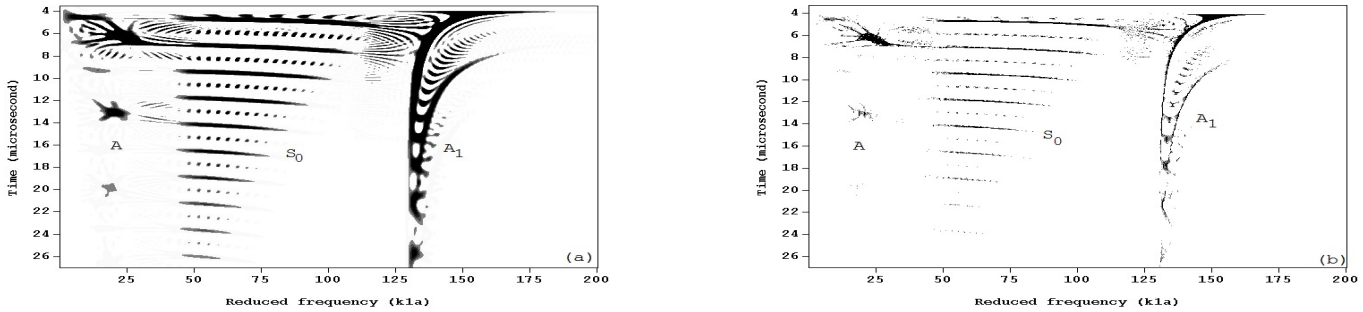

Figure 6: Time-frequency images of the Aluminum tube (b/a=0.95): (a) of SPWV and (b) of RSPWV, θ = 180°

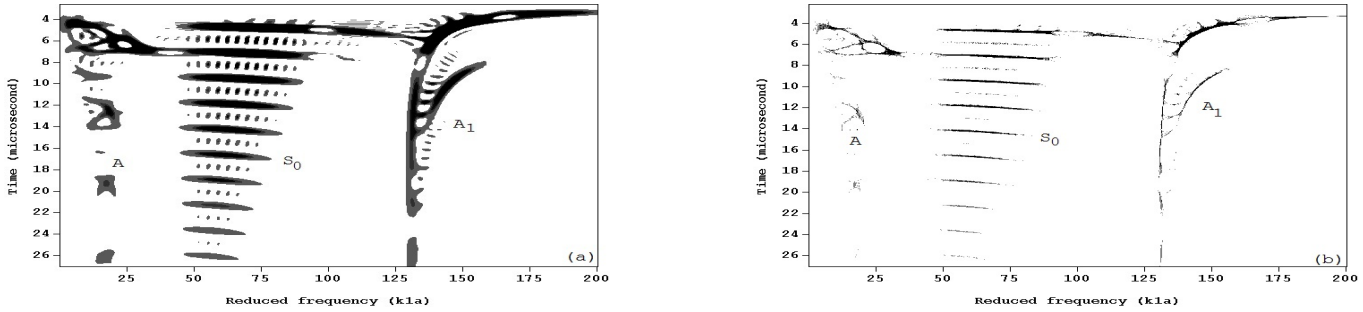

Figure 7: Time-frequency images of the Aluminum tube (b/a=0.95): (a) of SPWV and (b) of RSPWV, θ = 170°

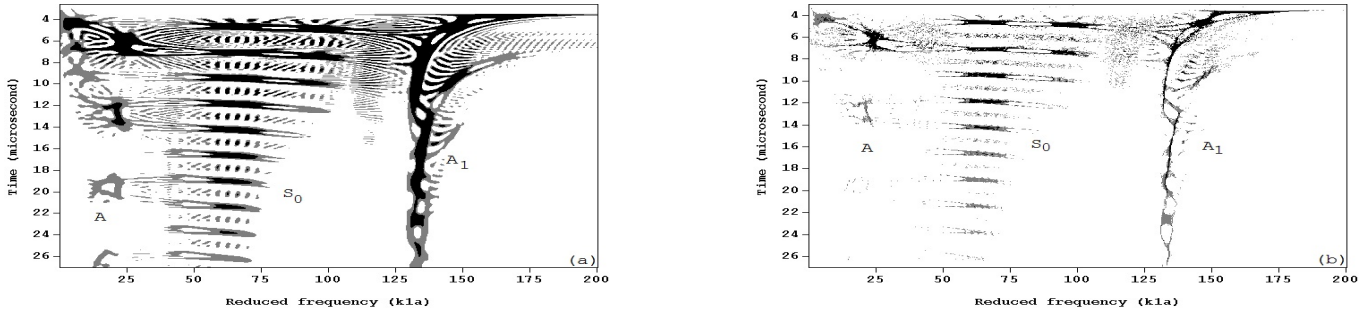

Figure 8: Time-frequency images of the Aluminum tube (b/a=0.95): (a) of SPWV and (b) of RSPWV, θ = 160°

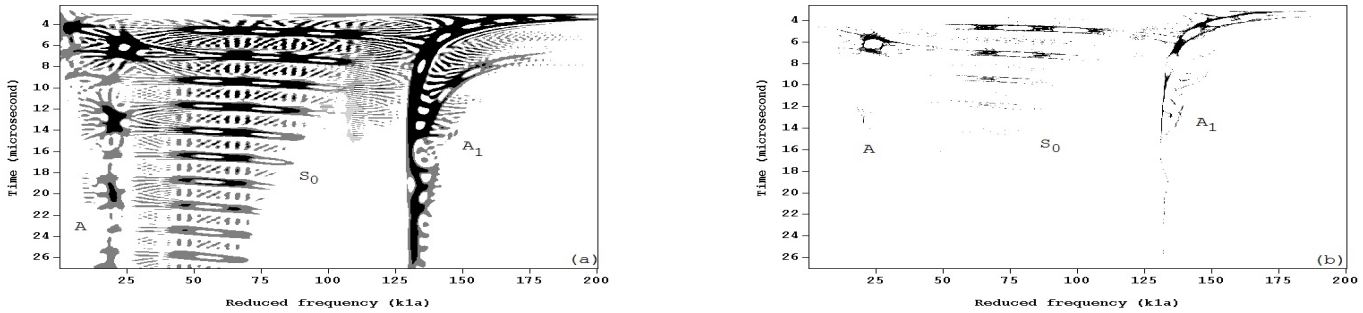

Figure 9: Time-frequency images of the Aluminum tube (b/a=0.95): (a) of SPWV and (b) of RSPWV, θ = 150°

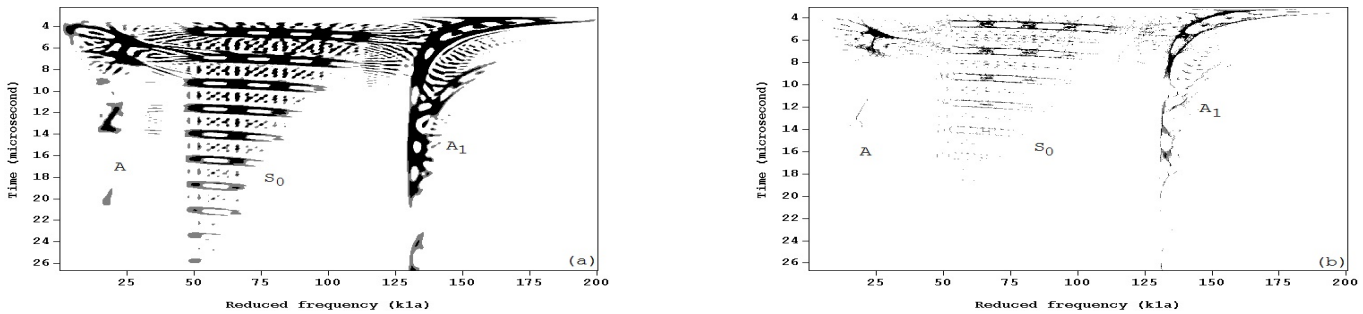

Figure 10: Time-frequency images of the Aluminum tube (b/a=0.95): (a) of SPWV and (b) of RSPWV, θ = 140°

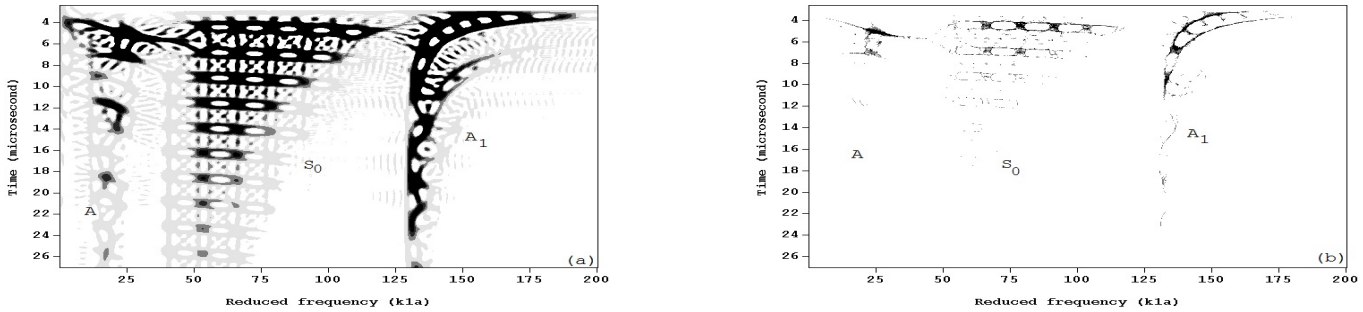

Figure 11: Time-frequency images of the Aluminum tube (b/a=0.95): (a) of SPWV and (b) of RSPWV, θ = 130°

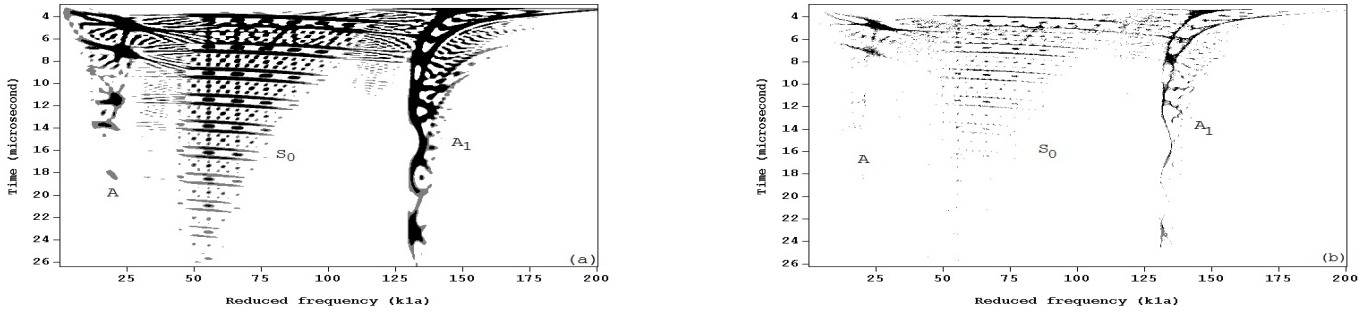

Figure 12: Time-frequency images of the Aluminum tube (b/a=0.95): (a) of SPWV and (b) of RSPWV, θ = 120°

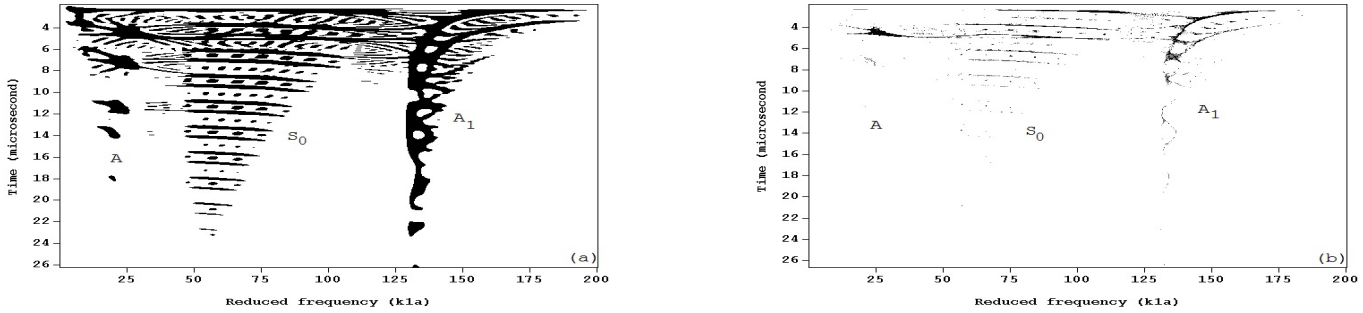

Figure 13: Time-frequency images of the Aluminum tube (b/a=0.95): (a) of SPWV and (b) of RSPWV, θ = 110°

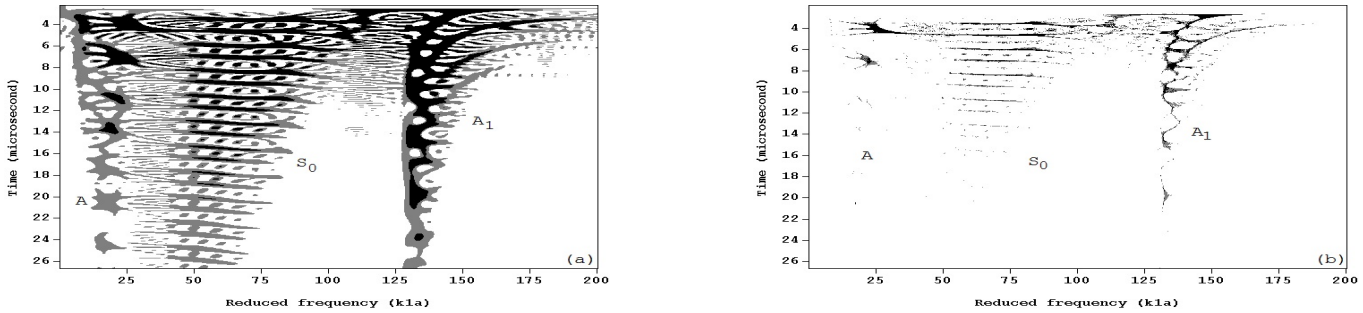

Figure 14: Time-frequency images of the Aluminum tube (b/a=0.95): (a) of SPWV and (b) of RSPWV, θ = 100°

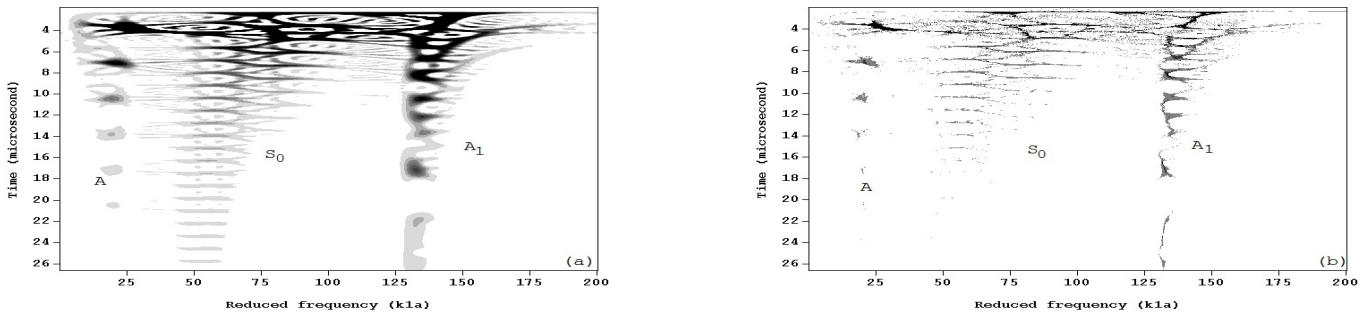

Figure 15: Time-frequency images of the Aluminum tube (b/a=0.95): (a) of SPWV and (b) of RSPWV, θ = 90°

From these time frequency images we could go out with the following points:

- The evolution of the time-frequency contents for the backscattering acoustic pressure from $\theta = 0°$ to $\theta = 90°$ is as almost the same as this evolution between $\theta = 90°$ and $\theta = 180°$.
- On the time-frequency plane we observe that each component of the wave packets A, S_0 and A_1 go to duplicate and the delay between the duplicate and its original is become more and more large when the azimuthal angle varied from $\theta = 180°$ to $\theta = 90°$.
- The backscattering pressure is always the contribution of the Scholte-Stoneley wave (A), the symmetric wave S_0 and the antisymmetric wave A_1.
- The frequency range and the cutoff frequency of different wave packets remain unchanged.

5 Conclusion

The present work shows the importance of the study jointly in time and frequency. The study of the backscattering acoustic pressure by the elastic tube under normal incidence, using the time-frequency representation demonstrates that each wave in the wave packets of the elastic waves (A, S_0 and A_1) show for the azimuthal angle $\theta = 180°$ (respectively $\theta = 0°$) are duplicated. The time delay between each duplicated wave and its original is increased progressively when the azimuthal angle varied from $\theta = 180°$ to $\theta = 90°$ (respectively from $\theta = 0°$ to $\theta = 90°$).

The comparison of SP and SPWV representations shows on one hand that the SP gives the time-frequency representations exclude of the interference terms but the broadening spectrum problem is the greatest inconvenient of this representation. On the other hand the SPWV provide the time-frequency representations with more localization than the SP, but is suffered from interference terms. The reassigned SPWV (RSPWV) allows to obtain the time-frequency images with the highest resolution and localization.

Moreover of the possibility to trick the evolution of the frequential contents of the elastic waves as a function of time, the time-frequency representation allows us to extract the relevant features (cutoff frequency, the phase velocities,...) which are used to characterize the target.

References

[1] M. Kempf, O. Skrabala, V. Altstad, Acoustic emission analysis for characterisation of damage mechanisms in fibre reinforced thermosetting polyurethane and epoxy, *COMPOS. PART. B-ENG.* **56**, 477-483 (2014).

[2] A. Dariouchy, E. H. Aassif, D. Décultot, G. Maze, Acoustic characterization and prediction of the cut-off dimensionless frequency of an elastic tube by neural networks, *IEEE. Trans. Ultrason. Ferroelectr. Freq. Control.* **54**, 1055-1064 (2007).

[3] J. Jiang, F. Gu, R. Gennish, D. J. Moore, G. Harris, A. D. Ball, Monitoring of diesel engine combustions based on the acoustic source characterisation of the exhaust system, *MECH. SYST. SIGNAL. PR.* **22**, 1465-1480 (2008).

[4] L. Flax, L. Dragonette, H. Überal, Theory of elastic resonance excitation by sound scattering, *J. Acoust. Soc. Amer.* **63**, 723-731 (1978).

[5] J. L. Izbicki, G. Maze, J. Ripoche, Influence of the free modes of vibration on the acoustic scattering of a circular cylindrical shell, *J. Acoust. Soc. Amer.* **80**, 1215-1219 (1986).

[6] G. Maze, Acoustic scattering from submerged cylinders. MIIR Im/Re: Experimental and theoretical study, *J. Acoust. Soc. Amer.* **89**, 2559-2566 (1991).

[7] G. Maze, J. L. Izbick, J. Ripoche, Resonances of plates and cylinders: Guided waves, *J. Acoust. Soc. Amer.* **77**, 1352-1357 (1985).

[8] J. Ripoche G. Maze, J. L. Izbicki, A New Acoustic Spectroscopy: Resonance Spectroscopy by the MIIR, *Journal of Nondestructive Evaluation,* **5**, 69-79 (1985).

[9] N. D. Veksler , *Resonance Acoustic Spectroscopy* , Springer Series on Wave Phenomena, Springer-Verlag Berlin Heidelberg, **11**, (1993).

[10] W. Gao, C. Glorieux, J. Thoen, Study of circumferential waves and their interaction with defects on cylindrical shells using line-source laser ultrasonics, *J. Appl. Phys.,* **9**, 6114-6119 (2002).

[11] G. Maze, F. Léon, F. Lecroq, D. Décultot, H. Überall, Nature de l'onde d'interface de Scholte sur une coque cylindrique, *JOURNAL DE PHYSIQUE IV,* **4**, 849-852 (1994).

[12] G. Maze, F. Léon, J. Ripoche, H. Überall, Repulsion phenomena in the phase velocity dispersion curves of circumferential waves on elastic cylindrical shells, *J. Acoust. Soc. Am.,* **105**, 1695-1701 (1999).

[13] P. L. Marston, Negative group velocity Lamb waves on plates and applications to the scattering of sound by shells, *J. Acoust. Soc. Am.,* **113**, 2659-2662 (2003).

[14] L. Cohen, *Time-Frequency Analysis*, Prentice Hall, Englewoods Cliffs, NJ, (1995).

[15] P. Flandrin, *Time-Frequency/Time-Scale Analysis, Wavelet Analysis and Its Applications*, Academic Press, San Diego, (1998).

[16] P. Flandrin, *Temps-fréquence*, second edition, Herm Paris, (1998).

[17] P. Flandrin, F. Auger, E. Chassande-Mottin, Time-frequency reassignment: from principles to algorithms, *in: P.-S. Antonia (Ed.), Applications in Time-Frequency Signal Processing,* 179-203 (2003).

[18] E. Chassande-Mottin, F. Auger, P. Flandrin, On the statistics of spectrogram reassignment vectors, *Multidim. Syst. Signal Process,* **9**, 355-362 (1998).

[19] F. Auger, P. Flandrin, Improving the readability of time-frequency and time-scale representations by the reassignment method, *IEEE Trans. Signal Process,* **43**, 1068-1089 (1995).